

PHOTORESIST METROLOGY AND MICROCALORIMETRY USING AN ULTRACOMPLIANT MICROMACHINED SCANNING THERMAL PROBE

Joo-Hyung Lee¹, Mo-Huang Li¹, and Yogesh B. Gianchandani^{1,2}

¹Department of Electrical and Computer Engineering, University of Wisconsin, Madison, WI, USA

²EECS Department, University of Michigan, Ann Arbor, MI, USA

ABSTRACT

This paper reports on the detection of nano-scale chemical variations in photosensitive polymers using scanning thermal probes fabricated from polyimide and metal thin films on a silicon substrate. The high thermal insulation achieved by these probes permits the measurement of thermal conductance variations $<10^{-11}$ W/K. The probes are mechanically very compliant, with a typical measured spring constant of 0.082 N/m. Lateral spatial resolution of <50 nm, topographic resolution of <1 nm and thermal resolution of <1 mK are demonstrated. An open loop interface circuit and a feedback controlled one that provides constant temperature operation are demonstrated and compared. The probes are used to measure the glass transition temperature and map undeveloped latent images in high resolution UV photoresist.

I. INTRODUCTION

Scanning thermal microscopy can be a significant asset in ULSI lithography research. Its applications include mapping the latent image of exposed but undeveloped photoresist (PR) to measure photo-acid generation and diffusion independently from the developing step, as well as measuring the variation in the glass transition temperature (T_g) with line width to estimate the impact of feature size on resist chemistry [1]. Thermal probes have also been used for data storage and other applications [2,3]. To best meet the needs for many applications, probes must have low spring constant to prevent damaging the soft materials, and provide spatial resolution <100 nm. These requirements cannot be fulfilled by using the commercially available wire probe which is made of bent bare wires, and has a high spring constant (5 N/m), limited spatial resolution, and no particular isolation [4].

We have previously reported thermocouple and bolometer probes fabricated by 6-7 mask surface micromachining processes using polyimide as the shank material, and the application of these probes for temperature mapping, sub-surface imaging, and the measurement of glass transition temperature in photoresists [5,6]. The use of polyimide not only makes the probes very compliant, but also provides very high thermal isolation, which minimizes the thermal loading of the sample and makes possible the detection of very small changes in thermal conductance. This paper reports on applying these probes to ULSI lithography research, particularly for mapping the latent image of exposed but undeveloped PR to measure photo-acid

generation (PAG) and diffusion independently. Within this context it also compares the performance of two different types of interface circuits that we have developed for these probes.

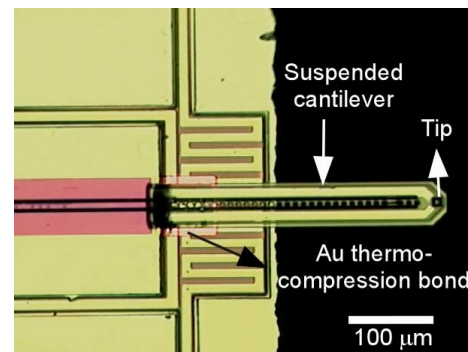
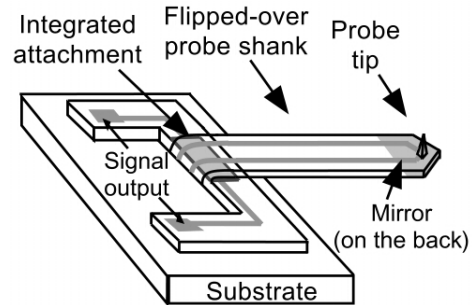


Fig. 1: Schematic and optical micrograph of the ultracompliant scanning thermal probe.

II. FABRICATION

The basic structure of the probe is similar to that reported in [5,6], with a thin film bolometer sandwiched between two layers of polyimide that form a cantilever (Fig. 1). At one end of the cantilever the metal thin film protrudes through an opening in lower polyimide layer, where it is molded into a pyramidal tip by a notch that was anisotropically wet-etched into the substrate (Fig. 2). A tip diameter of about 50 nm can be achieved by sharpening the notch by non-uniform oxide growth [7]. The tip and a portion of the probe shank are then released from the substrate by etching an underlying sacrificial layer. The released length is then folded over to extend past the die edge for clearance. It is held in place by a thermocompression bond across a thin film of gold (Cr/Au: 200/2500 Å) that is deposited on top of the polyimide. This method retains the flatness of the probe and significantly increases yield. This layer also serves as a mirror to permit simultaneous operation of the probe as an AFM. Typical dimensions of

the probes after assembly are 350 μm length, 60 μm width, and 3 μm thickness with Cr/Ni (200/1000 \AA) or Cr/Au (200/2000 \AA) for the tip, and Cr/Au (200/2000 \AA) for the lead, which provides bolometer resistance about 40 Ω .

III. DEVICE OPERATION AND INTERFACE

The topography and thermal conductance of a sample can be mapped simultaneously as shown in Fig. 3. As the probe scans the sample surface, the topographic image is produced by detecting the reflected laser beam from a mirror placed on the probe while a mechanical feedback loop maintains a constant contact force. The probe resistance, which is altered by the heat exchange between the tip and the sample, is used to map the thermal conductance.

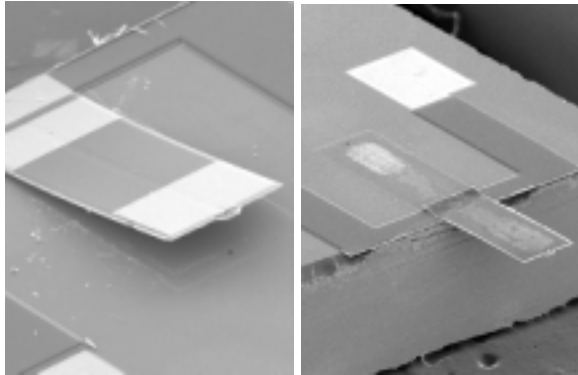


Fig. 2: (a-left) Scanning electron micrograph of released probe 185 μm wide and 460 μm long; (b-right) SEM image of flipped-over probe.

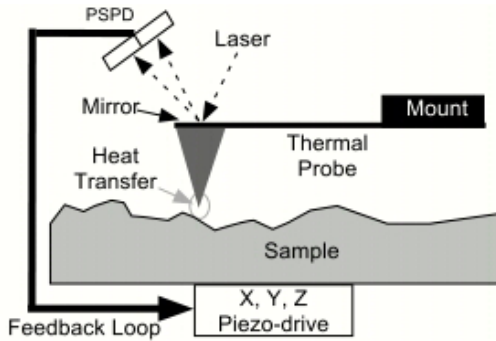


Fig. 3: The operation of scanning thermal microscopy.

Over small temperature fluctuations, the electrical resistance of most conductors can be linearly related to the temperature by:

$$R_p = R_o \cdot [1 + TCR \cdot (T - T_0)] \quad (1)$$

where R_o is the resistance at temperature T_0 and TCR is the temperature coefficient of resistance. Hence, for better performance of the probe, the resistance change in the probe shank should be minimized during the scan. This can be done by reducing the parasitic resistance of the leads, by

increasing the thickness and the width as shown in Fig. 4.

When heat loss through probe shank is small and scanning speed is low compared to the thermal time constant, the probe tip temperature T_p is linearly proportional to change in sample thermal conductance (Fig. 5a). Therefore, probe resistance can be monitored when operating in constant power mode. In constant temperature mode, power is supplied to keep the probe temperature constant, which allows us to control probe temperature (Fig. 5b). This constitutes a second feedback loop.

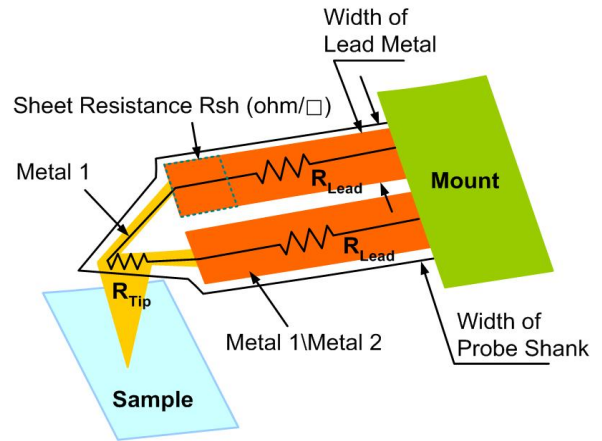


Fig. 4: Schematic of micromachined bolometer showing the lead resistance that is minimized.

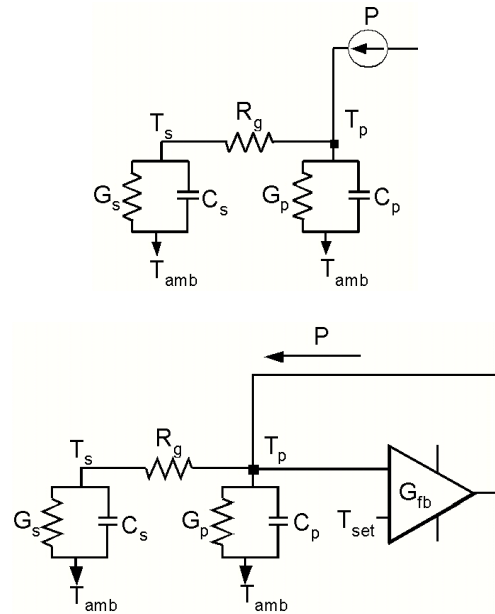


Fig. 5: Equivalent diagram for thermal sensing system operating: (a-upper) in a constant power mode; (b-lower) in a constant-temperature mode. G_s and C_s are thermal conductance and capacitance of sample, respectively. R_g is thermal resistance of gap between probe tip and sample surface. T_s and T_p are the average temperature of sample surface and probe, respectively. T_{amb} is the ambient temperature.

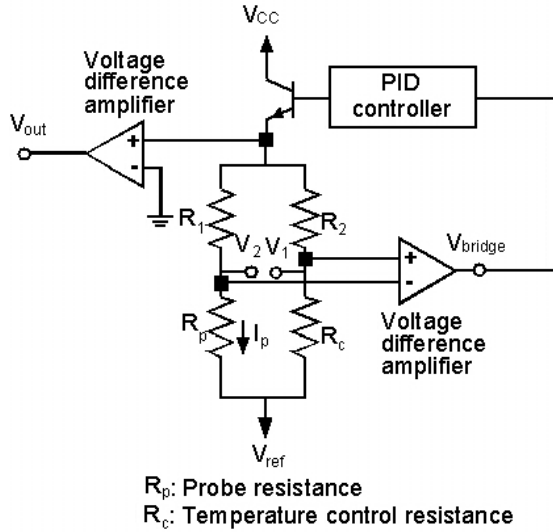
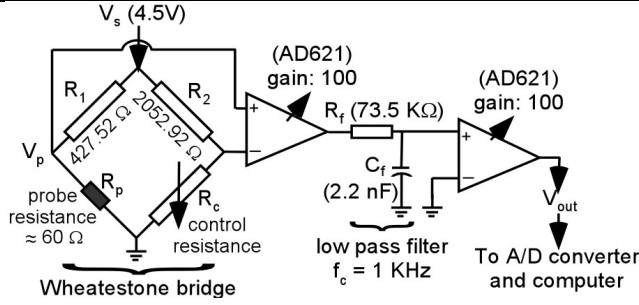


Fig. 6: Interface circuits for (a-upper) constant power mode and (b-lower) constant temperature mode.

Figures 6 (a) and (b) show interface circuits used to operate the probe in constant power mode and in constant temperature mode, respectively. The former is an open loop interface circuit which includes a Wheatstone bridge, two gain stages providing combined amplification of 10^4 , and a low pass filter with cut-off frequency of 1 kHz to reduce noise. The output voltage (V_{out}) is plotted in thermal scans. The probe tip temperature change (ΔT_p) can be calculated from the output voltage change (ΔV_{out}), which is:

$$\Delta T_p \cong \Delta V_{out} (R_1 + R_p)^2 / (10^4 \cdot V_s R_1 R_p \cdot TCR) \quad (2)$$

A ΔV_{out} of 100 mV corresponds to a ΔT_p of 5.657 mK calculated using the voltage and resistance values shown in Fig. 6(a), and the measured temperature coefficient of resistance (TCR) of 3640 ppm/K for the Cr/Au bolometer. The full scale ΔT_p is indicated for all thermal scans presented in this paper. Before a scan, this circuit is adjusted to balance the Wheatstone bridge with the probe in contact with the sample by adjusting the control resistor (R_c) to make the resistance ratio of R_c/R_2 equal to R_p/R_1 so that the output voltage is as close as possible to 0 V. The circuit used for constant temperature operation operates in closed loop (servo-controlled) mode (Fig. 6b), and offers a faster response

time. In this circuit, R_1 and R_2 , are 280 Ω and 2000 Ω , respectively. The probe resistance R_p was 36 Ω at room temperature. In the PID controller, the proportional gain is 1, whereas the integration gain is 20,000.

In scanning a Si wafer with an ultra-thin photoresist layer of thickness comparable to the scan tip diameter, the heat transfer between the probe tip and silicon substrate can be modeled as that through a cylinder. The heat loss (P_s) to the silicon substrate can be expressed as:

$$P_s = (T_p - T_0) \cdot A_0 \cdot k_s / H \quad (3)$$

where T_p is the probe tip temperature, A_0 is the tip-sample contact area, k_s is the thermal conductivity of photoresist, and H is the photoresist thickness. The silicon substrate is a large heat sink, effectively with a fixed temperature T_0 . The thermal conductance image obtained from V_{out} contains both topographic and thermal conductivity information.

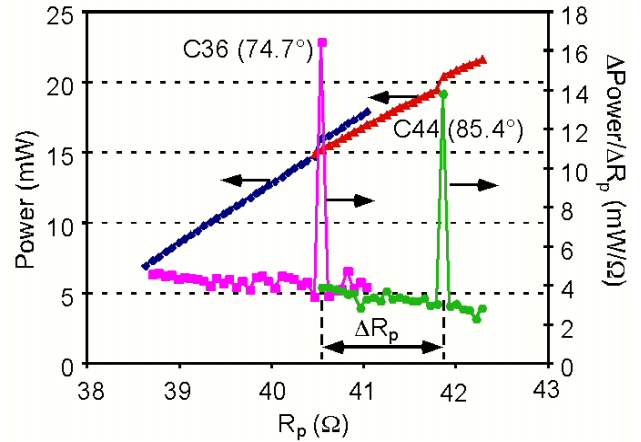


Fig. 7: Calibration of bolometer probe using closed loop interface circuit and melting-point-known materials

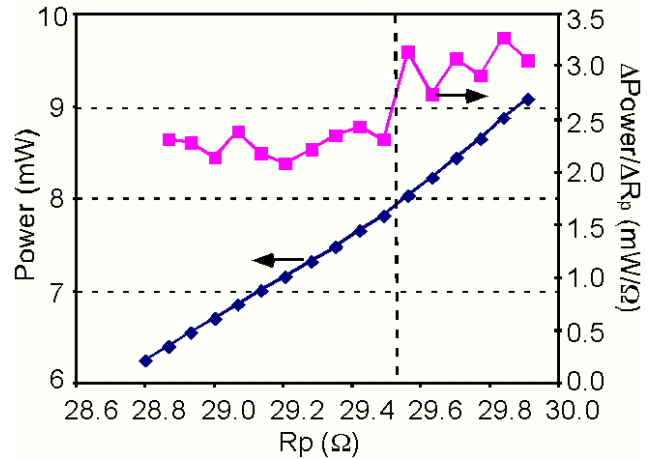


Fig. 8: Glass transition temperature (T_g) measurement for PR1827 using closed loop interface circuit of Fig. 6b.

IV. MEASUREMENT RESULTS

In constant temperature mode, calibration is necessary to determine the TCR of the bolometer (Fig. 6b). This can be performed either at the wafer level before the probe is released from the substrate wafer, or prior to usage when all the assembly is complete. One way to perform the latter calibration is with the help of melting point standards, as shown in Fig. 7. Thus, using [13]:

$$TCR \cong \frac{\Delta R_p}{R_o \cdot k \cdot (T_{M1} - T_{M2})} \quad (0 < k < 1) \quad (4)$$

where T_{M1} and T_{M2} are melting temperatures of known materials, in this case, C_{36} and C_{44} . The thermal probe can also be used to measure glass transition temperature as shown in Fig. 8. In this sense it is essentially behaving as a microcalorimeter. If this parameter is shown to change with feature size, it will indicate that the resist chemistry is being affected by the dimensions, which may be indicative of the scaling limit of its chemistry.

The spring constant of a 250 μm long, 50 μm wide, and 3 μm thick probe shank measured by using a built-in function in the Topometrix™ scanning system is 0.082 N/m, which is about 10 \times and 50 \times lower compared those reported in [2,4]. This allows contact mode scanning of soft materials such as photoresist patterns with feature size of 500 nm even without the mechanical feedback that keeps the tip-sample pressure constant as illustrated in Fig. 4. A scan obtained without this feedback and using the open loop circuit of Fig. 6a is shown in Fig. 9. The output voltage drops as the probe is scanned across the higher thermal conductivity material (silicon), because the heat loss from the tip to sample increases, which reduces the tip temperature, and the corresponding probe resistance.

Figures 10 and 11 compare the response of the probe when operated in a conventional scanning mode (i.e. which includes the mechanical feedback of Fig. 4), but with the two circuits of Fig. 6. The latter also includes the topographic image obtained from the laser pick-off.

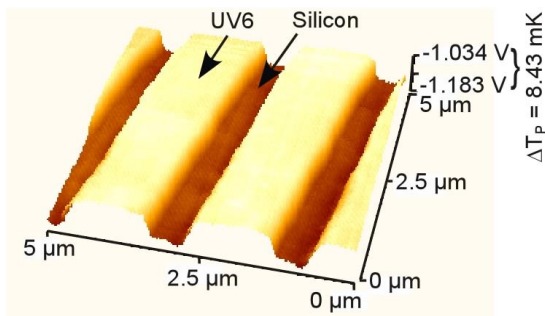


Fig. 9: Thermal image of developed UV6 photoresist sample with thickness of 350 nm. Scan was obtained without z-direction feedback using the circuit of Fig. 6a.

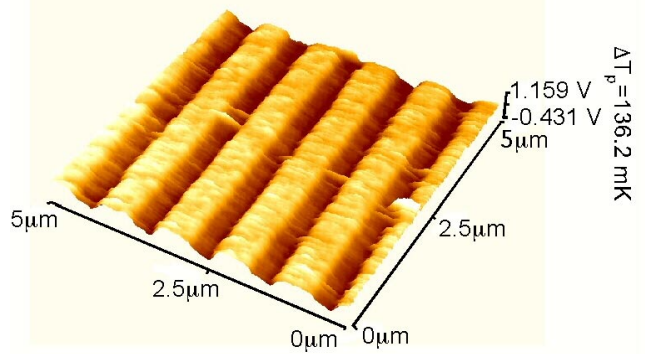


Fig. 10: Thermal image of 350 nm thick developed UV6™ using the DC open loop interface circuit of Fig. 6a.

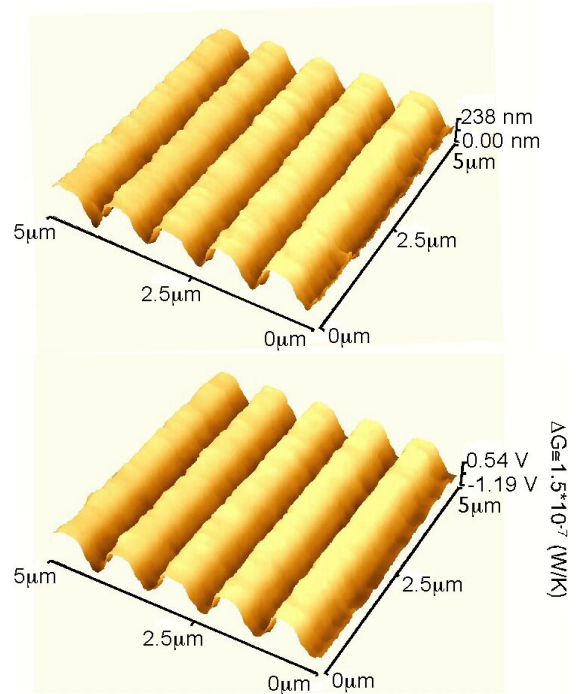


Fig. 11: Topographic (upper) and thermal (lower) images of 1000 nm pitch lines of developed 350 nm thick UV6™ using DC closed loop interface circuit of Fig. 6b.

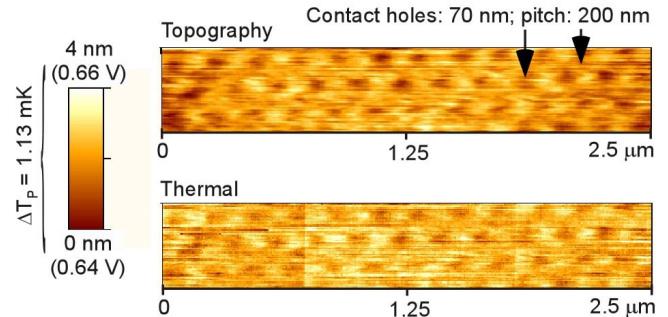


Fig. 12: Topographic (top) and thermal (bottom) images of exposed but undeveloped UV113™ photoresist contact holes of 70 nm obtained with the circuit of Fig. 6a.

Figure 12 shows the topographic and thermal images of exposed but undeveloped UV113™ photoresist patterned with critical dimension of 70 nm and 200 nm pitch. Comparing the topographic and thermal images of partial developed UV113™ photoresist sample (Fig. 13), it is evident that the thermal probe has a lateral spatial resolution of <50 nm. The topographical resolution is <1 nm. The interface circuit of Fig. 6a is sensitive enough to detect a tip temperature change only 1.13 mK.

The positive tone chemically amplified photoresist UV6™ by Shipley, which is suitable for ultra-narrow ULSI linewidths, behaves as shown in Fig. 14 [8]. Unlike standard PR and PMMA, a photoacid generated by exposure permits thermolysis of the backbone polymer during the post exposure bake (PEB), which changes the solubility of the exposed regions of the resist and releases isobutylene. The photoresist thickness decreases in exposed areas where released isobutylene is evaporated during PEB. It is, therefore, important to control the PEB conditions to suppress the acid diffusion for critical dimension control when using chemical amplification resist systems.

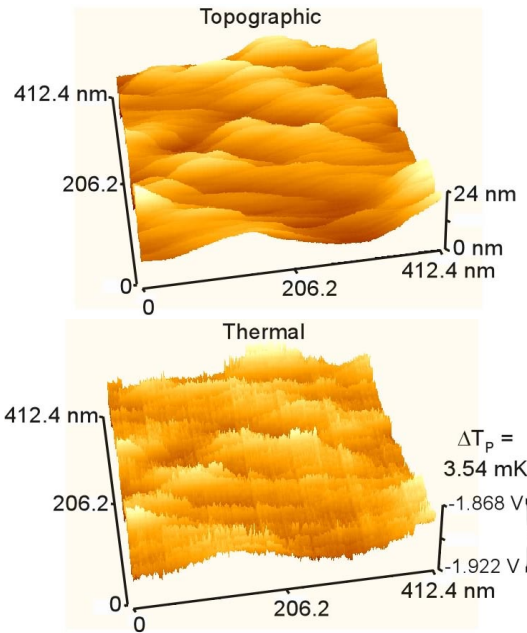


Fig. 13: Topographic (top) and thermal (bottom) images of partial developed UV113™ photoresist obtained with the circuit of Fig. 6a showing sub-50nm spatial resolution.

Figure 15 shows the topographic and thermal linear scans of a trench in exposed but undeveloped Shipley UV6™ photoresist. As the duration of the 130°C PEB increases from 45 s to 360 s, both the topographic height change (Δh) and ΔV_{out} increase. However, the most significant change in Δh occurs in the 45-90 s period, whereas the most significant change in ΔV_{out} occurs in the 180-360 s period. As noted above, the Δh is due to the release of isobutylene and depends on the acid concentration and the reaction rate of photoresist

backbone deprotection. The “v” shape profiles of exposed regions are due to the Gaussian distribution of the e-beam source of dose profile, and hence, the acid concentration [1]. As the PEB time increases, the “v” shape profile widens due to the acid diffusion. However, since the acid diffusion constant, which depends on the process conditions [9], is only about 50 nm²/s for UV6™ [10], this change is very small (~10 nm) [11], particularly when compared to the 500 nm width of the exposed portion. Since the recommended PEB condition for 130 °C is 90 s, the longer PEB times may deplete the photoresist backbone, minimizing subsequent changes in topography. In contrast, other chemical changes may lead to the ΔV_{out} increase during the 180-360 s period.

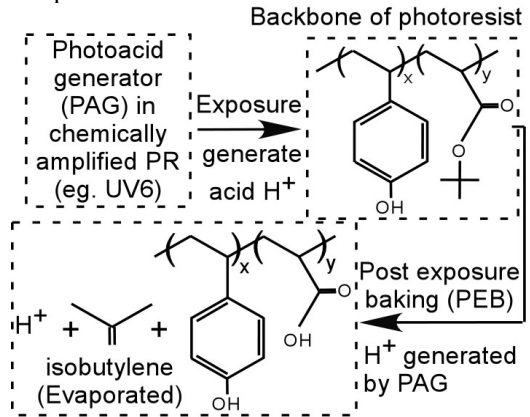


Fig. 14: In UV6™, PAG acid deprotects the backbone during PEB for subsequent dissolution in the developer.

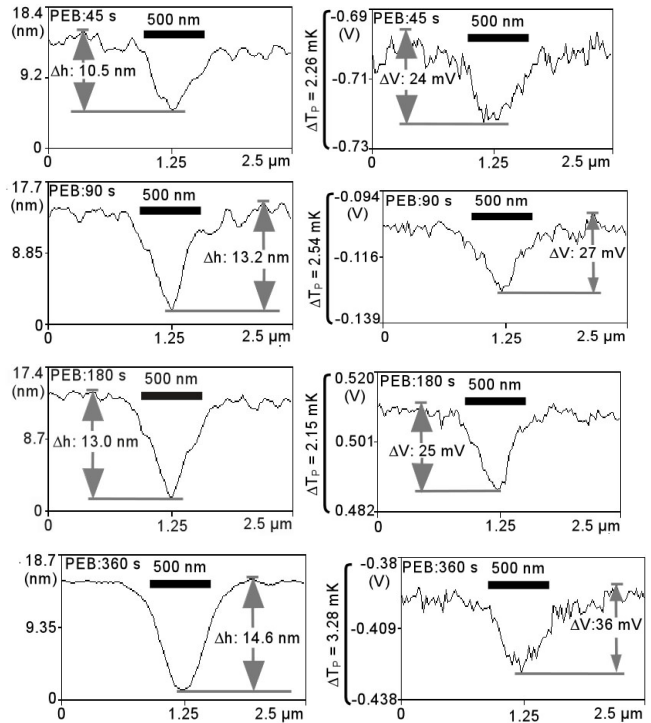


Fig. 15: Topographic (left) and thermal (right) line scans of a latent image in UV6™ with varying PEB time at 130°C.

Table I: Performance of the polyimide probe.

Performance	Open-Loop Circuit	Closed-Loop Circuit
Tip Diameter	≈50 nm	
Lateral Spatial Resolution	<50 nm	
Topographical Resolution	<1 nm	
SNR for UV6 350 nm	5.11	6.48
ΔR Resolution	<0.25 mΩ	NA
Tip Temperature Resolution @ SNR=2	<1.2 mK	< 1.0 mK
Detectable Thermal Cond. Change (W/K)	7.0×10^{-11}	5.0×10^{-12} @ SNR=2

V. CONCLUSION

This effort has addressed the development and applications of polyimide shank thermal probes fabricated by a 6-mask process. Typical probe dimensions are 250-500 μm length, 50-200 μm width, and 3 μm thickness. The probes are ultra-compliant with a spring constant of 0.082 N/m, which can be further reduced by changing the material and/or dimensions. They can be operated without z -direction feedback, even when scanning soft materials. The probe offers lateral spatial resolution of <50 nm, topographical resolution of <1 nm, and tip temperature resolution of <1 mK. Two types of interface circuits were explored, showing that high resolution can be obtained both in an open loop and closed loop operating conditions. The latter facilitates the constant temperature scanning mode, which is particularly helpful for measurements of glass transition temperature. The probe was also used to scan exposed but undeveloped photoresist samples, to study the acid diffusion in photoresist during post-exposure bake. A summary of the measured operating limits is presented in Table I.

ACKNOWLEDGEMENTS

The authors thank Dr. Leo Ocola for supporting the UV113™ photoresist sample. This work was funded in part by the Semiconductor Research Corporation contract # 98-LP-452.005. The Center for NanoTechnology, University of Wisconsin-Madison, is supported in part by DARPA/ONR grant # MDA 972-00-1-0018, and # MDA 972-99-1-0013. The Synchrotron Radiation Center, University of Wisconsin-Madison, at which some of the experimental facilities are located, is operated under NSF award # DMR-0084402.

REFERENCES

- [1] L.E.Ocola, D.Fryer, P.Nealey, J.dePablo, F.Cerrina, and S. Kämmer, "Latent image formation: Nanoscale topography and calorimetric measurements in chemically amplified resists," *J. Vac. Sci. Technol. B*, 14(6), pp. 3974-9, 1996.
- [2] P.Vettiger, et al., "The "Millipede"-More than one thousand tips for future AFM data storage," *IBM J. Res. Develop.*, 44(3), pp. 323-40, 2000.
- [3] A.Majumdar, "Scanning thermal microscopy," *Annu. Rev. Mater. Sci.*, 29, pp. 505-85, 1999.
- [4] TM Microscopes, www.tmmicro.com, probe model# 1615-00.
- [5] M.-H.Li, J.J.Wu, Y.B.Gianchandani, "Surface micromachined polyimide scanning thermocouple probes," *J. Microelectromech. Sys.*, 10(1), pp. 3-9, 2001.
- [6] M.-H. Li, Y.B. Gianchandani, "Microcalorimetry applications of a surface micromachined bolometer-type thermal probe," *J. Vac. Sci. Technol. B*, 18(6), pp. 3600-3, 2000.
- [7] S.Akamine, C.F.Quate, "Low temperature thermal oxidation sharpening of microcast tips," *J. Vac. Sci. Technol. B*, 10(5), pp. 2307-10, 1992.
- [8] H.Ito, "Chemically amplified resists: past, present, and future," *SPIE Vol. 3678*, pp. 2-12, 1999.
- [9] T.Itani, H.Yoshino, S.Hashimoto, M.Yamana, N.Samoto, K. Kasama, "A study of acid diffusion in chemically amplified deep ultraviolet resist," *J. Vac. Sci. Technol. B*, 14(6), pp. 4226-8, 1996.
- [10] D.Kang, E.K.Pavelchek, C.Swible-Keane, "The accuracy of current model descriptions of a DUV phototresist," *SPIE*, vol. 3678, pp. 877-90, 1999.
- [11] T.H.Fedynyshyn, J.W.Thackeray, J.H.Georger, M.D. Denison, "Effect of acid diffusion on performance in positive deep ultraviolet resists," *J. Vac. Sci. Technol. B*, 12(6), pp. 3888-94, 1994.
- [12] R.L.Warters, O.L.Stone, "Histone protein & DNA synthesis in HeLa cells after thermal shock," *J. Cell. Phys.*, 118, pp. 153-60, 1984.
- [13] H.S.Carlsaw, J.C.Jaeger, *Conduction of Heat in Solids*, 2nd, Oxford, pp. 18-24, 146-154, 1959